Journal of
Bioengineering & Biomedical Science
ISSN: 2155-9538

Tomostar, J Bioengineer & Biomedical Sci 2016, 6:4
DOI: 10.4172/2155-9538.1000199

Review Article Open Access

A Novel Blood Pump Design and Characterization

Michael Tomostar*

Russian Institute of Technology, St Petersburg, Russia

Abstract

The aim of the European project Nephron+ is the design of a wearable artificial kidney device. This paper is focused on the design of the corresponding ultralow-hemolysis continuous- operation blood pump. Accurate specifications and operating principle of the pump are determined. A first nonoptimal configuration of a linear electromechanical actuator which will be used to pump the blood is designed. Its prototype is presented along with the corresponding driving electronic circuit. Finally, based on the measurements, the actuator is optimized, and the final design and first experimental results are presented.

Keywords: Actuators; Efficiency; Hemolysis; Medical control systems; Microcontroller; Pumps

Introduction

The kidneys serve the body as a natural filter of the blood, as they remove wastes which are diverted to the urinary bladder [1]. In producing urine, the kidneys excrete wastes such as urea and ammonium, and they are also responsible for the absorption of water, glucose, and amino acids, keeping the body's internal equilibrium of water and minerals.

Dialysis

In the case of kidney disease or failure (which is referred to as nephropathy), an artificial replacement should be made, which means that an external device should remove waste from the blood. This artificial filtering process is called dialysis. It is regarded as a "holding measure" until a renal transplant can be performed (or, sometimes, as the only supportive measure in patients for whom a transplant would be inappropriate). However, this "holding" function should often last for a long time, as the need for a kidney is much higher than the offer: In Switzerland in 2009, the mean waiting time was 700 days [2].

The main type of the dialysis is the hemodialysis. It consists in removing the waste by circulating blood outside the body through an external filter, called a dialyzer, that contains a semipermeable membrane. The patient's blood is pumped through the blood compartment of a dialyzer. The blood flows in one direction through the membrane, and a special liquid, called dialysate, flows in the opposite direction. The countercurrent flow of the blood and dialysate maximizes the concentration gradient of solutes between the blood and dialysate, which helps to remove more waste from the blood.

The main problem with dialysis is that the patient needs to be placed in the hospital and that it is typically performed three times per week, with 4 h for each treatment. In addition, each treatment requires 120 L of dialysate. All this is, of course, related to a huge cost of treatment.

Envisaged artificial kidney

In order to significantly improve the patient's quality of life and reduce the costs, the goal of the European project Nephron+ [3], which started in April 2010 and will last for four years, is to design a wearable device to replace the bulky dialyzer. Its main property will be the continuous blood filtering, which is much more beneficial for the patient's health, with a significantly reduced quantity of dialysate. The participants in the project are, among many others, the Swiss Center for Electronics and Microtechnics (CSEM) from Neuchatel, Switzerland, and the Ecole Polytechnique Federale de Lausanne, Switzerland. The device is to be supplied from batteries and carried by the patient. Hence, the device can be regarded as a wearable artificial kidney. This will be the first device of this type at the market.

State of the art

Many different studies have been done on wearable or implantable rotary blood pumps for ventricular assistance devices, which may be either centrifugal [4,5] axial [6-8]. They show that the required blood flow and pressure drop are different from the requirement of a blood pump needed for a hemodialysis system. Indeed, the blood flow for a kidney device is usually more than 30 times lower. Also, the required pressure in standard utilization is two times higher. Due to these important differences, the mentioned rotary pump does not suit for our use. Even if the rotary blood pump may reach the required pressure drop for an artificial kidney, it would require a higher rotational speed, which would significantly increase the hemolysis rate.

Lee et al. studied a valveless pulsatile blood pump [9]. It is shown that this kind of pump provides better results than conventional units in terms of hemolysis, which is an extremely important characteristic in continuous extracorporeal blood circulation.

Other candidates for the pump are also analyzed. The electroosmotic pumps can generate the flow rate which is too small for the presented application, and in addition, they require a too high voltage (typically 100 V). The syringe-type pumps may generate clotting problems.

Finally, the references which served as inspiration for the presented project are [10-14]. They present various configurations of pumps, for blood and other liquids. The design of a pump for a portable renal replacement system. The principle is different from that which will be presented in this paper [15]: Several cams sequentially compress fingers, which compress flexible tubes, thus eliminating valves. The pump volume of 150 cm^3 and the achieved flow rate of 100 mL/min are similar to the performance which will be presented in this paper.

***Corresponding author:** Michael Tomostar, Russian Institute of Technology, St Petersburg, Russia, Tel: 7(812)4949339; E-mail: mark.dingliu@gmail.com

Received: August 08, 2016; **Accepted:** August 19, 2016; **Published**: August 30, 2016

Citation: Tomostar M (2016) A Novel Blood Pump Design and Characterization. J Bioengineer & Biomedical Sci 6: 199. doi:10.4172/2155-9538.1000199

Citation: Tomostar M (2016) A Novel Blood Pump Design and Characterization. J Bioengineer & Biomedical Sci 6: 199. doi:10.4172/2155-9538.1000199

Artificial Kidney and its Blood Pump

Principle of operation

The principle of operation of the artificial kidney device is shown in Figure 1. It is a hemodialysis machine, in which the patient's blood is continuously, using a blood pump, circulated through a semipermeable extracorporeal membrane and returned to the patient (blood circuit in red in Figure 1).

The opposite side of the same membrane is washed with an electrolyte solution (dialysate) containing the normal constituents of plasma water. Diffusion (osmotic pressure) and convection (hydrostatic pressure) are the two mechanisms causing a flow of water and dissolved substances from the blood to the dialysate compartment. A special pump is used to circulate the dialysate (dialysate circuit in blue in Figure 1). The undesired molecules are removed from the dialysate using a filter with nanoparticles in a sorbent unit. The aim of this paper is to show the procedure of the design of the blood pump. For cost reasons, the pump must be reusable without excessive maintenance.

Blood pump specifications

The mean blood pressures in arteries and in veins are $P_a = 100$ mmHg and $P_v = 40$ mmHg, respectively (750 mmHg = 100 kPa). In addition, the semipermeable membrane will be opposed to the blood flow, which means that it will generate a pressure drop. The corresponding value is estimated to $P_m = 450$ mmHg. Hence, the blood pump should compensate the total pressure drop, which is therefore estimated to $P_p = P_m + P_v - P_a = 390$ mmHg = 52 kPa. Note that the positive difference $P_a - P_v$ will "help" the pump during its operation. The maximal necessary flow rate of the blood is estimated to 200 mL/min, which means that $Q_p = 3.3 \times 10^{-6}$ m^3/s. The necessary mechanical power to be provided by the pump is hence $P_p\, Q_p = 0.172$ W. If we suppose the efficiency of 10%, the necessary electrical power to be consumed by the pump is approximately 1.7 W. To complete the specifications, the pump volume and mass should not overpass 140 cm^3 and 400 g, respectively.

Blood pump additional requirements

Apart from the "mechanical" specifications concerning the pumping of blood, some other considerations should be taken due to the specificity of the blood. At first, blood is a complicated fluid. It contains red blood cells (RBCs) which contain the hemoglobin.

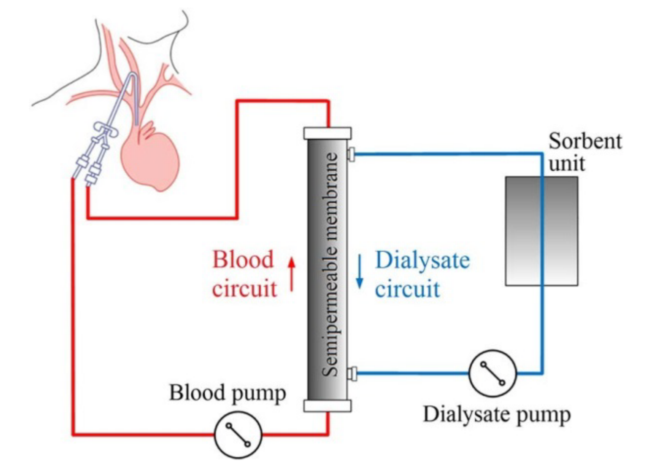

Figure 1: Principle of operation of the artificial kidney device.

The RBC can be easily destroyed by one of the following three factors: mechanical force, sudden variation of the pressure, or the temperature. Concerning the first two factors, their critical values are not easy to estimate. Concerning the temperature, it should not overpass 45°C [16].

The process of RBC destruction is called hemolysis: When an RBC is destroyed, the hemoglobin is freed. It means that the increased concentration of hemoglobin means the increased hemolysis. The normalized index of hemolysis (NIH) is a clinical measure of hemolysis measured as the concentration of hemoglobin in the blood. Its value should not overpass 100 mg per 100 L of pumped blood.

In addition, if the blood stays immovable during a short time, there is a risk of thrombosis (formation of blood clot). Hence, the geometry of the pump should be made taking this fact into consideration: It should not contain "corners" in which the blood can stay without moving. All the mentioned requirements are too difficult to take into account during the pump design. Only the measurements on the pump prototype will give responses if those requirements are met. Finally, the pump should be "bloodtight" which means that no blood can escape and (equally important) that the air cannot enter. An air bubble can have catastrophic consequences for the patient [17].

Pump Configuration and Operation

Pump configuration

After a preliminary study, it is decided that an optimal pump configuration for this application is a linear peristaltic pump with two elastic tubes, as shown in Figure 2. As it is peristaltic, it enables to know the blood flow rate without a sensor which significantly improves the system reliability and cost. The pump contains four actuators (A, B, C, and D) which move in the vertical direction. Using two tubes, when the actuator is to switch from one to another end (extreme) vertical positions, the elastic force of the closed tube will help the movement toward the position where another tube should be closed. It is also important to point out that the actuator couples A and C, and B and D, operate simultaneously and in the opposite direction: When one from the couple goes up, another goes down and *vice versa*.

In the closed state, the tube opening will be zero (tube completely

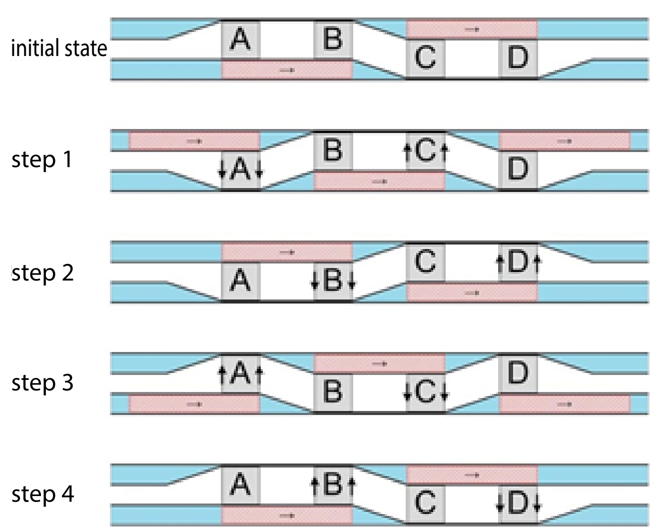

Figure 2: Pump configuration and its operation in four steps [13].

pinched). In the open state, the tubes will not be left completely without external force: A remaining force will keep the tube opening equal to 50% of its diameter in the free state. This will help the tube to restore its shape during the refilling at the inlet of the pump, making the pump less sensitive to inlet pressure.

Actuator specifications

The chosen tube is made of silicone elastomer and produced by Maagtechnic. Its internal diameter is 8 mm; the wall thick- ness is 1 mm. This industrial tube does not fulfill the medical norms (at first hemocompatibility), but it will be used for the pump first prototype. The final prototype is intended to be made using the tubes made of Tygon 3350 by Saint-Gobain (which fulfills the norms, more precisely ISO 10993 guidelines for contact with blood), but due to nonstandard dimension, it has a delivery time too long to wait for the first prototype.

The elastic force of the chosen tube is experimentally measured. Finally, the necessary profile of the force which one actuator should generate is given in Figure 3. The position values of $+2/0/-2$ mm correspond to high-end/mean/low-end positions, respectively.

The force is shown for the actuators B and C from Figure 2, as they should generate higher force than A and D. Indeed, suppose that the actuator is in the low-end position and starts its moving toward the high-end position (such as B between steps 3 and 4). It is the low pressure (and force F_{lp}) in the lower tube which helps the movement and the high pressure (and force F_{hp}) in the higher tube which is opposed to the movement. Therefore, the difference $F = F_{hp} - F_{lp}$ is shown in Figure 3 as the force F which should be generated by the actuator over the stroke of 4 mm.

After the calculations which take into account the tube dimensions and the necessary blood flow rate, it is obtained that each actuator should press the tube at its length of 12 mm with the frequency of 2 Hz (so the sequence in Figure 2 repeats twice each second).

Actuator Preliminary Design

Actuator configuration

Using electromagnetic actuators is the best compromise between simplicity of construction, power consumption, and maintenance [14].

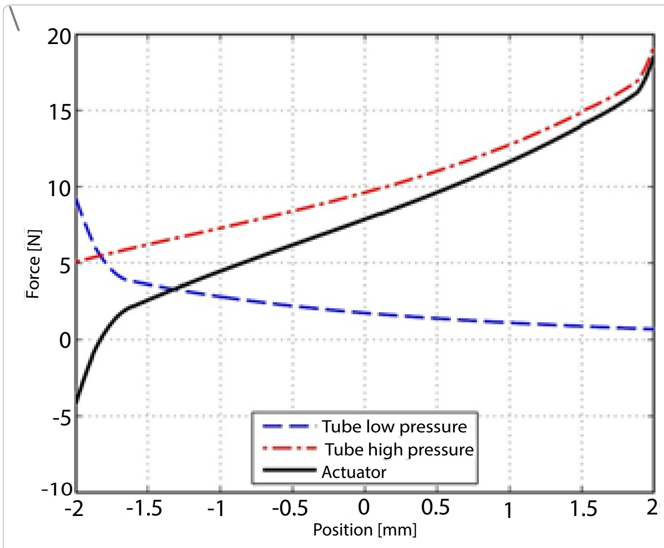

Figure 3: Necessary force that should be generated by one actuator.

Four candidates (1, 2, 3, and 4) are taken into account for the actuator configuration (Figures 4 and 5). Each of them is analyzed using a simple analytical model and a finite- element model (FEM) commercial software package.

After a quick preliminary analysis (the results will not be presented here), the configurations 1 and 2 are eliminated, as their constant force profile along the stroke does not correspond to the force requirement for the actuator (Figure 3). Thus, in order to generate a significant force in extreme positions, those actuators should have a huge volume (typically twice the volume required by specifications). The configurations 3 and 4 have an advantage of having an important reluctant force at the end of the stroke, which allows maintaining the tube closed without current.

Finally, after the first calculations, it turned out that the configuration 3 is not suitable, as its two windings require significant volume and mass. Hence, the configuration 4 is chosen, which contains one winding.

Actuator modeling

The actuator geometry with all its design parameters is shown in Figure 6. The electromagnetic analytical model is based on the analysis of the equivalent magnetic circuit represented in Figure 7. The force is

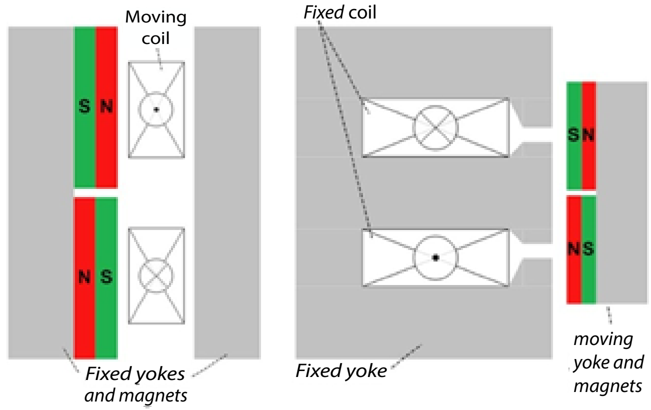

Figure 4: Actuator configurations (left) 1 and (right) 2.

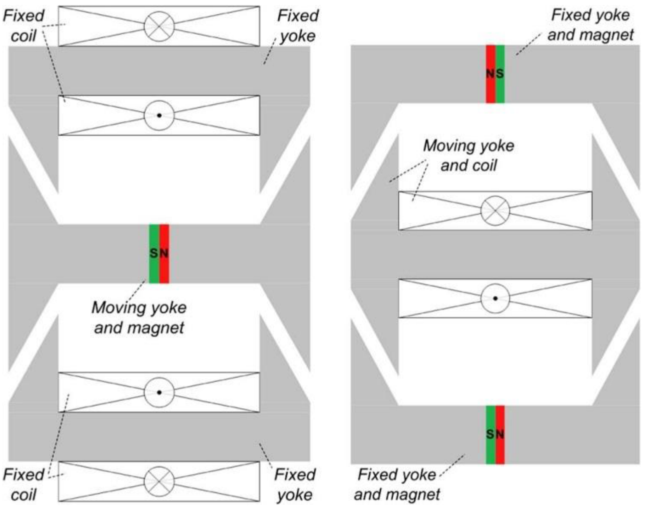

Figure 5: Actuator configurations (left) 3 and (right) 4.

determined by the derivation of magnetic energy W_{mag} by using the formula $F_y = -dW_{mag}/dy$, with y as the mover vertical position. The iron is assumed to be linear; this assumption is provided by the optimization process as it will be shown later: The magnetic flux density is limited so that the iron stays far from the saturation.

In Figure 7, $\Lambda_{Iron\ 1}$, $\Lambda_{Iron\ 2}$, and $\Lambda_{Iron\ 3}$ represent the reluctances of the iron; Λ_i is the internal reluctance of the magnets; Λ_h and Λ_l represent the (variable) reluctances of the higher and the lower air gaps, respectively; Θ_m and Θ_{coil} are the magnetic potentials (magnetomotive forces) of the magnets and the coil, respectively; and Φ_{mh}, Φ_{ml}, and Φ_{coil} are the resulting magnetic fluxes flowing in the magnetic circuit branches.

All of the previous reluctances are calculated using the geo- metrical parameters of the actuator and the magnetic properties of the iron and the magnet. The flux leakage in the air gap, represented in Figure 8, is neglected in the presented model, and only the reluctance enclosed by the red rectangle is taken into account. Again, the reluctances of the air gaps highly depend on the vertical position (y) of the mover.

Finally, the magnetic energy W_{mag} is calculated as a function of the mover position. The energy is calculated in each part of the magnetic circuit (magnets, air gaps, and iron yokes), by knowing that the energy volume density is given by $w_{mag} = (BH)/2$. It is worth noting that the main part of the energy is contained in the air gaps and in the magnets. Finally, all those energy components are added, and the total energy is derived to obtain the force as already explained.

Actuator first prototype

The first actuator prototype is not a result of optimization. Instead, the values of its parameters are quickly chosen to more or less satisfy the specifications, with the goals to verify the actuator electromagnetic analytical model, to generate the actuator thermal analytical model, and, finally, to refine the specifications. Based on all this, the second prototype will be the result of a detailed optimization. The first actuator prototype is shown in Figures 9 and 10. Its mass is 124 g.

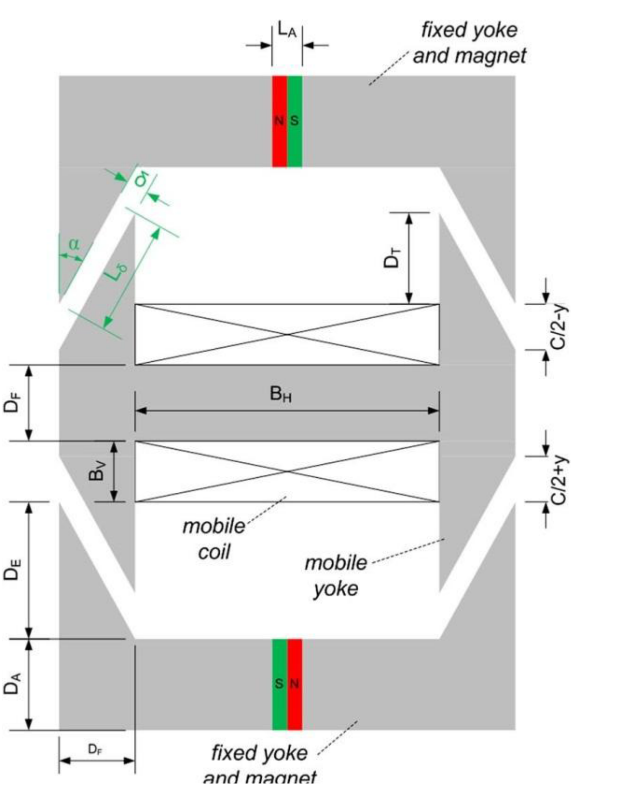

Figure 6: Chosen actuator configuration with its geometrical parameters.

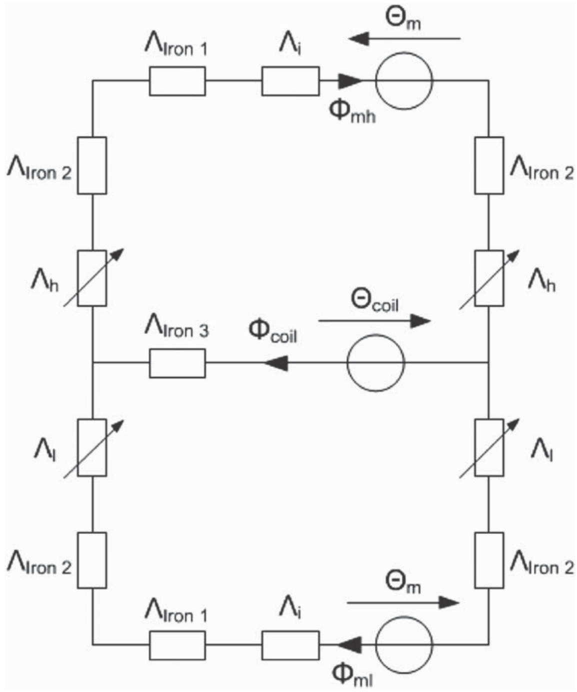

Figure 7: Equivalent magnetic circuit of the actuator.

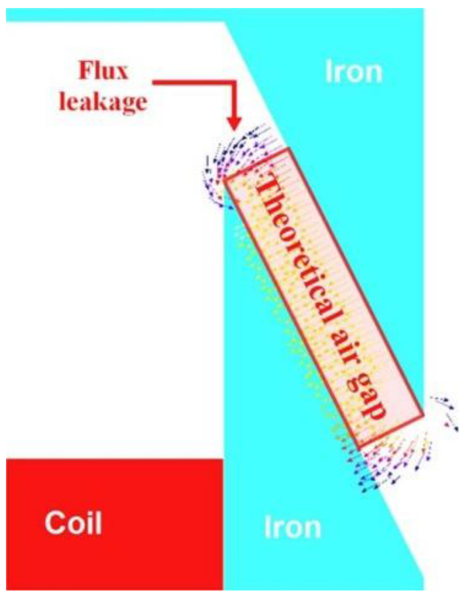

Figure 8: Simulated magnetic flux lines in the air gap.

Measurements on the actuator first prototype

In order to verify the electromagnetic analytical model, the force is measured. A constant current of 1.1 A is injected in the winding. In addition, the actuator is simulated using a FEM commercial software which calculates the force. Figure 11 shows the corresponding results and confirms that the electromagnetic analytical model is correct. The differences between the results for the position above 1 mm are due to the saturation of the ferromagnetic parts. In order to be able to generate a simple thermal analytical model, a constant power of 2.92 W is dissipated in the winding, and the thermal steady state is established. Figure 12 shows the temperature measured using a thermal camera.

Obviously, the whole mover can be regarded as an isothermal body. Using the measured temperatures and dissipated power, the thermal resistance between the mover and surrounding air is obtained as 23.1 K/W. By supposing that this resistance corresponds to the natural convection over the mover surface, the corresponding convection coefficient is 14.7 W/(m^2 · K). This value will be taken to calculate the thermal resistance in the simple thermal model which will be used to optimize the actuator. It is important to note here that only the

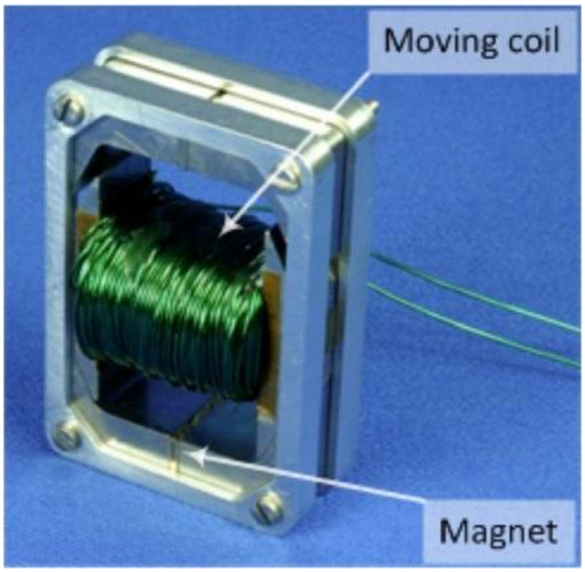

Figure 9: First actuator prototype.

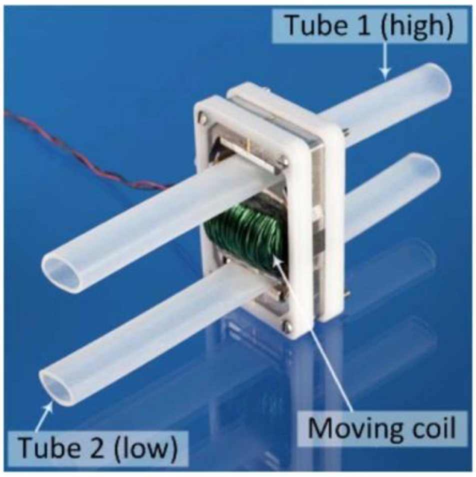

Figure 10: First actuator prototype with two tubes.

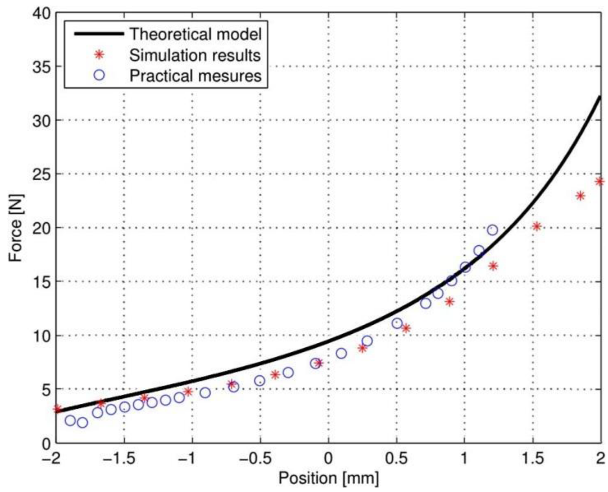

Figure 11: Force generated by the actuator: Comparison between the analytical model, FEM, and experimental results.

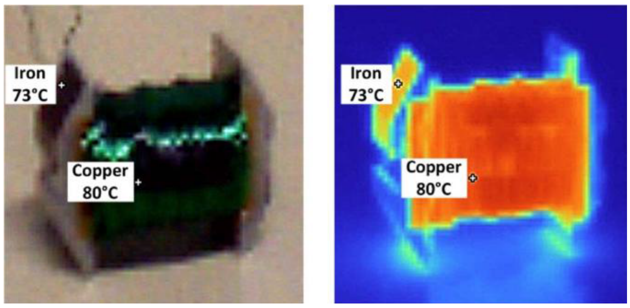

Figure 12: Actuator temperature measured by a thermal camera (the ambient temperature is 22.2° C).

winding surface temperature will be calculated in the model. This value has to be limited to 45°C according to the specifications. The winding insulation will not be a critical element in this case as it can support the temperature of 80°C.

Control Electronic Circuits

The control system for the operation of the blood pump is composed of a central computer, four power cards, and four position measurement cards (one per actuator). The central computer communicates with the power cards via the port RS485. The power card (Figure 13) contains a microcontroller STM32F103 which gives the ON/OFF commands for the power transistors according to the pulse width-modulation logic. The actuator is driven by the MC33887 integrated H-bridge. Also, each power card receives a signal from the position measurement card. The position is determined by measuring two capacitances: between the upper yoke and mobile yoke and between the lower yoke and mobile yoke. In order to do this, the position measurement card sends two rectangular voltage signals to the upper and lower mobile yokes and detects the voltage of the mobile yoke. After demodulation, the resulting analog signal, which is proportional to the position, is sent to the power card.

Actuator Optimal Design

The final goal is to obtain the optimal actuator configuration using

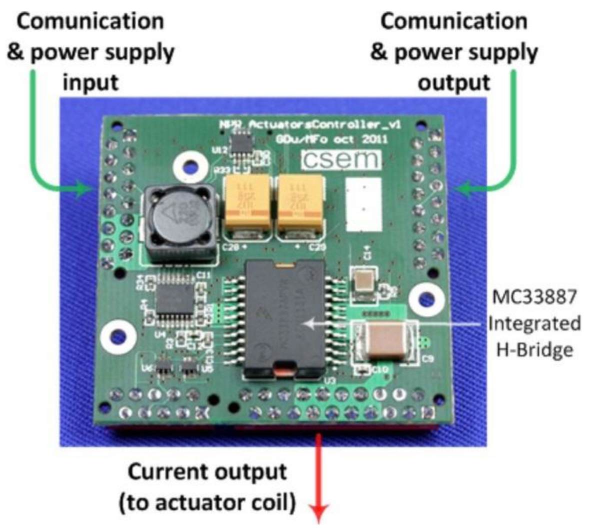

Figure 13: Power card.

the verified analytical models. The optimization will be performed using the software package ProDesign [18] and is inspired by [19].

Required force profile

The actuator force has to satisfy the required profile (Figure 3), which means that this profile will impose some constraints for the optimization. As the optimization tool is not able to accept this profile as one constraint, it is decided to "sample" the profile in eight points. Those points (values of position and force) are presented in Table 1. The force corresponding to the point 8 has to be achieved without current, i.e., only by the reluctant force (Table 2 and 3).

Optimization

In order to perform the optimization, the software ProDesign needs at first the actuator analytical model. Concerning the constraints, eight points from Table 1 impose eight constraints. In addition, the flux density in the iron is limited to 1.5 T; the temperature is limited to 45°C as required by specifications. As the specifications impose 400 g as the maximal pump mass, it means that the maximal actuator mass is limited to 100 g. The value of the current density is left free, in order to be adapted to provide the necessary force for each point.

Therefore, a complete theoretical model including electromagnetic force calculation in eight points and a thermal model is introduced in the optimization software; the chosen optimization function is simply the volume of the actuator. Thus, the optimization software varies all the parameters simultaneously to minimize the volume accordingly to the defined constraints. To perform the optimization, the software applies an advanced sequential quadratic programming algorithm, which is an iterative method for nonlinear optimization.

Finally, Tables 1 and 2 present the optimal actuator configuration. The iron is Armco; the magnet remanence is 1.4 T. The optimal actuator drawing is shown in Figure 14. The set of four actuators is presented in Figure 15, and the whole system is presented in Figure 16.

Experimental Results

The very first experiments on the optimal actuator show promising results. Figure 17 shows the necessary actuator force (imposed by the specifications) compared to the simulation and experimental results and the corresponding current injected in the coil. All the three forces match well.

Concerning the operation of the whole pump, the first experiments are performed using a constant current of 1.2 A (maximal value from Figure 17). In that case, the pump generates the flow rate of 150 mL/min (0.75 L is pumped in 5 min) and the pressure drop of 38 kPa.

Point	Position [mm]	Force [N]
1	-1.5	2.6
2	-1	4.5
3	-0.5	6.2
4	0	7.9
5	0.5	9.7
6	1.0	11.7
7	1.5	14.1
8	1.9	18.3

Table 1: Points from the force profile.

Variable	Value [mm]
BV	4.9
BH	33.4
DF	4.3
DE	6.9
DA	5.0
LA	1.0
DT	7.0

Table 2: Optimal actuator configuration.

Parameter	Value
mass	104 g
power	1.17 W
temperature	42 deg
volume	34.7 cm^3

Table 3: Optimal actuator main parameters.

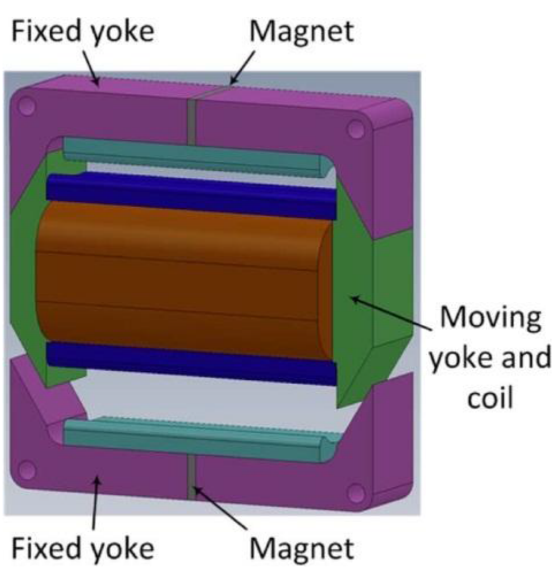

Figure 14: Optimal actuator.

Citation: Tomostar M (2016) A Novel Blood Pump Design and Characterization. J Bioengineer & Biomedical Sci 6: 199. doi:10.4172/2155-9538.1000199

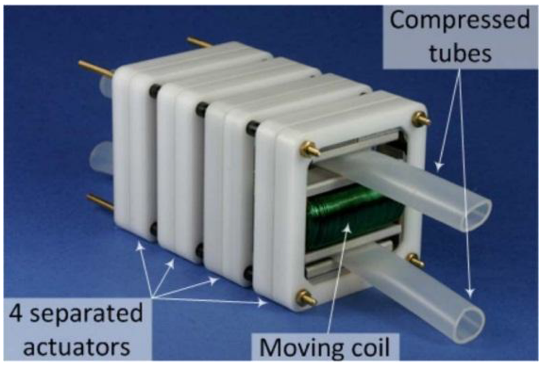

Figure 15: Set of four actuators.

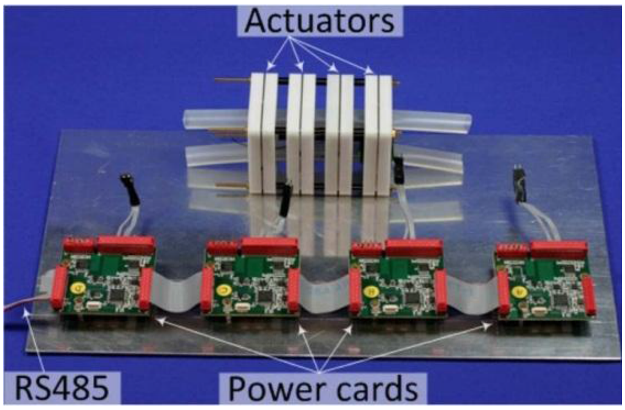

Figure 16: Whole system.

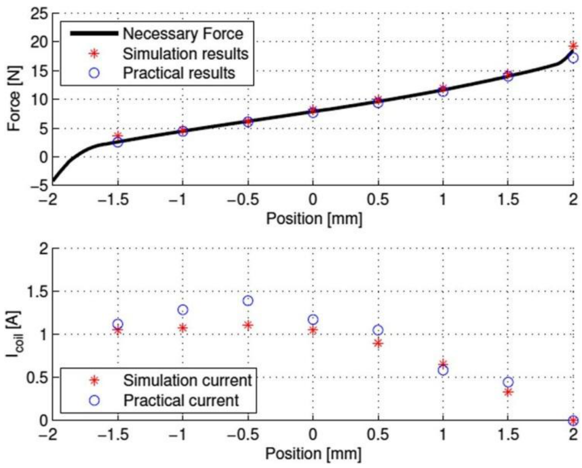

Figure 17: Optimal actuator force.

The required flow rate of 200 mL/min will be achieved by increasing the frequency above 2 Hz, and the required pressure of 52 kPa will be achieved by increasing the current.

Summary and Future Work

This paper has presented the design of a blood pump for a wearable artificial kidney device. The first experiments have shown that the pump satisfies the desired specifications in terms of rate of flow and pressure drop. The prototype is now ready for the next steps: measurement of NIH in a specialized laboratory. The project Nephron+ continues until April 2014. A first demonstrator containing the real-time microfluidic circuit board integrating the physical sensors, some actuators, and several filtering systems is now available [3]. The NIH measurement tests of the blood pump will start in February 2013.

The main drawback of the device is the noise which it generates. In the actual state, it cannot be used, as the noise would be annoying for the patient. In order to address this problem, the control algorithm will be modified for the actuator final version, so as to reduce the speed at closing of the tubes.

References

1. Kidney.
2. Swiss Confederation website.
3. ICT enabled Wearable Artificial Kidney and Personal Renal Care System. NEPHRON+ at the MobiHealth IEEE conference, Athens, November 2014.
4. Ertan M, Taskin KH, Fraser T, Zhang B, Gellman A, et al. (2010) Computational characterization of flow and hemolytic performance of the ultramag blood pump for circu- latory support. Artif Org 34:1099-1113.
5. Hijikata W, Sobajima H, Shinshi T, Nagamine Y, Wada S, et al. (2010) Disposable maglev centrifugal blood pump utiliz- ing a cone-shaped impeller. Artif Org 34: 669-677.
6. Pirbodaghi T, Weber A, Carrel T, Vandenberghe S (2011) Effect of pulsatility on the mathematical modeling of rotary blood pumps. Artif Organs 35:825-32.
7. Yang SM and Lin CC (2007) Performance of a single-axis controlled magnetic bearing for axial blood pump. Conf Rec 42nd IEEE IAS Annu Meeting.
8. Wang F, Wang J, Kong Z, Xu L (2003) A novel BLDC motor with passive magnetic bearings for blood pump application. Conf Rec 38thIEEE IAS Annu Meeting1429-1433.
9. Lee K, Mun CH, Lee SR, Min BG, Yoo KJ, et al. (2008) Hemodialysis using a valveless pulsatile blood pump. ASAIO J 54: 191-196.
10. Kim S, Hashi S, Ishiyama K (2012) Actuation of novel blood pump by direct application of rotating magnetic field. IEEE Trans Magn 48: 1869-1874.
11. Yang S, Huang M (2009) Design and implementation of a magnetically levitated single-axis controlled axial blood pump. IEEE Trans Ind Electron 56: 2213-2219.
12. Lim E, Dokos S, Cloherty SL, Salamonsen RF, Mason DG, et al. (2010) Parameter-optimized model of cardiovascular–rotary blood pump interactions. IEEE Trans Biomed Eng 57: 254-266.
13. Hu M, Du H, Ling S (2002) A digital miniature pump for medical application. IEEE/ASME Trans. Mechatronics 7: 519-523.
14. Pirbodaghi T, Asgari S, Cotter C, Bourque K (2014) Physiologic and hematologic concerns of rotary blood pumps: what needs to be improved? Heart Fail Rev 19: 259-266.
15. Kang J, Tamera S, Weaver JD, Ku DN, Rosenc DW (2011) Pump design for a portable renal replacement system. Biomed and Biotec Eng 2: 331-340.
16. Yeun J, Depner T (2005) Principles of Hemodialysis. Philadelphia, PA, USA: Elsevier.
17. Davenport A, Gura V, Ronco C, Beizai M, Ezon C, et al. (2007) A wearable haemodialysis device for patients with end-stage renal failure: A pilot study. Lancet 370: 2005-2010.
18. Design processing technologies.
19. Ji J, Zhao W, Liu G, Wang F (2012) High reliability linear drive device for artificial hearts. J Appl Phys 111.